*Carbohydrate Research*, 175 (1988) 1–15
Elsevier Science Publishers B.V., Amsterdam – Printed in The Netherlands


# THE CRYSTAL STRUCTURE OF GELLAN

RENGASWAMI CHANDRASEKARAN*, RICK P. MILLANE, STRUTHER ARNOTT,
*The Whistler Center for Carbohydrate Research and Department of Biological Sciences, Purdue University, West Lafayette, IN 47907 (U.S.A.)*

AND EDWARD D. T. ATKINS
*H. H. Wills Physics Laboratory, University of Bristol, Tyndall Avenue, Bristol BS8 1TL (Great Britain)*
(Received June 1st, 1987; accepted for publication, August 3rd, 1987)

ABSTRACT

Gellan is a nonsulfated, anionic, extracellular polytetrasaccharide secreted by the bacterium *Auromonas elodea*. It is potentially useful in the food industry because of its gel-forming properties. The molecular basis of these properties had been investigated by X-ray diffraction analysis of oriented fibers, but an exhaustive study by Upstill *et al.* in 1986 produced no molecular model with a remotely acceptable fit to the observed X-ray intensities. We describe here a successful re-examination of the crystal structure of gellan; the gellan chains have backbone conformations different from those previously considered. Two left-handed, 3-fold helical chains are organized in parallel fashion in an intertwined duplex in which each chain is translated half a pitch ($p$ = 5.64 nm) with respect to the other. The duplex is stabilized by interchain hydrogen bonds at each carboxylate group. There are two molecules in each trigonal unit cell ($a$ = 1.56 nm and $c$ = 2.82 nm).

## INTRODUCTION

Gellan is a linear, extracellular, anionic polysaccharide secreted by the bacterium *Auromonas elodea*. The native material, approximately 6% (by weight) *O*-acetylated, forms weak gels. Upon deacetylation, the aqueous solutions are highly viscous even at concentrations as low as 0.04%, and form stiff, brittle gels. Because gellan is nonsulfated, as opposed to such other commonly used texturing agents as carrageenan and agar, it may be more acceptable to the food industry.

Gellan has the tetrasaccharide repeating unit[1,2] →3)-β-D-Glc*p*-(1→4)-β-D-Glc*p*A-(1→4)-β-D-Glc*p*-(1→4)-α-L-Rha*p*(1→ and is schematically represented in Fig. 1. The quality of the early diffraction patterns[3,4] was not adequate for a detailed structural analysis. Recently, high-quality diffraction patterns from well oriented, polycrystalline specimens of the lithium salt have been obtained[5]. An X-ray diffraction study, however, provided no structural model consistent with the

*To whom correspondence should be addressed.

0008-6215/88/$ 03.50 

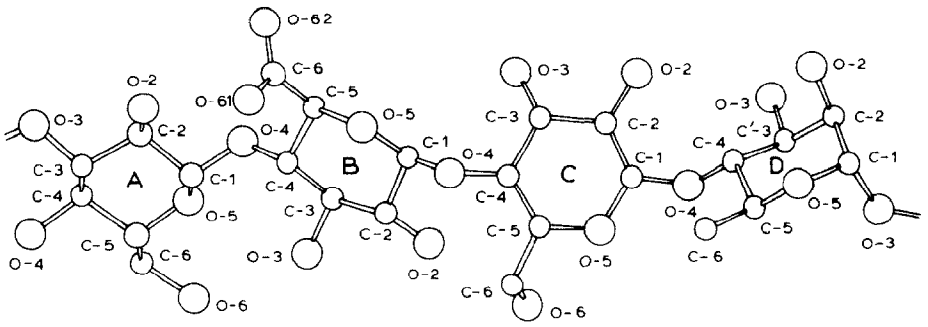


Fig. 1. Schematic representation of the chemical repeating-unit. [A, B, C, and D are β-D-glucose, β-D-glucuronate, β-D-glucose, and α-L-rhamnose, respectively.]

X-ray data[5]. This prompted the present re-examination of the structure of this potentially important polysaccharide.

The intensities of the Bragg reflections were measured by using digital-processing techniques. All possible molecular models were examined, using the Linked-Atom Least-Squares (LALS) procedure[6], establishing that gellan gum forms a half-staggered, parallel double-helix, similar to those of ι-carrageenan[7] and agarose[8].

## EXPERIMENTAL

*X-Ray intensity data.* — Well oriented, polycrystalline fibers of the lithium salt of deacetylated gellan gum give X-ray diffraction patterns of the kind shown in Fig. 2. This pattern was obtained from a calcited fiber, using radiation of wavelength 0.15418 nm from a high-flux synchrotron source at the SERC Daresbury Laboratory[5].

The diffraction pattern was digitized by using an Optronics P-1000 rotating-drum microdensitometer with a 100 μm raster. Background correction and structure amplitudes were determined as previously described[9,10].

*Model building, and joint X-ray-contact refinement.* — Molecular models of the polysaccharide chain constrained to have the appropriate observed helical symmetry and pitch were generated by using the linked-atom least-squares procedure[6]. Standard $^4C_1$ pyranose rings[11] for the one D-glucosyluronic and two D-glucosyl residues in the β-D-configuration, and a $^1C_4$ pyranose ring for the α-L-rhamnosyl residue[12] were used. The bond angle at each glycosidic bridge-oxygen atom was initially set to 116.5°. All hydrogen atoms were included in the models. The main conformational variables in the tetrasaccharide unit were the 8 glycosidic bridge torsion-angles and the 4 other rotations defining the hydroxymethyl, carboxylate, and methyl side chains. The pyranose rings were flexed in the final stages of X-ray refinement, and the subsidiary variables for each sugar residue were

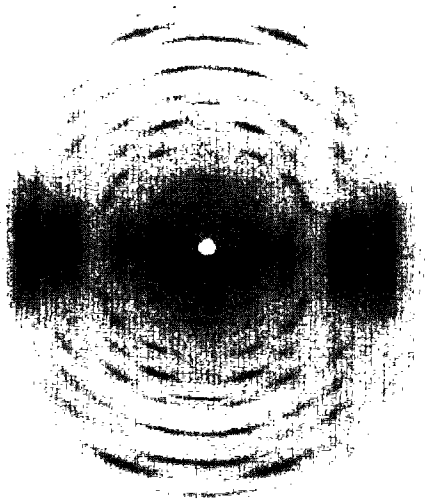

Fig. 2. X-Ray fiber diffraction pattern from an oriented and polycrystalline sample of the lithium salt of gellan.

the 6 ring conformation angles, 6 endocyclic bond-angles, and the glycosidic bridge bond-angle, each tethered to its respective, standard value. In addition, an X-ray scale factor, one or more packing parameters, such as the orientation ($\mu$) and axial displacement ($w$), expressed as a fraction of $c$, of a molecule in the unit cell, were also varied. The function minimized in the least-squares procedure is given by Eq. *1*.

$$\Omega = \Sigma\omega_m({}_oF_m - F_m)^2 + \Sigma e_i\Delta\theta_i^2 + \Sigma c_j\Delta d_j^2 + \Sigma\lambda_h G_h = X + E + C + L \qquad (1)$$

The first term $X$, optimizes the agreement between the observed and calculated structure amplitudes, and $\omega_m$ is the weight associated with the $m$th observation. The structure factors were calculated from the atomic scattering factors[13], modified to compensate for the presence of solvent surrounding the polyanions in the crystal[14]. The second term, $E$, ensures that the elasticated molecular variables (with weight $e_i$) are in their expected domains. The third term, $C$, optimizes the non-bonded and hydrogen-bond interactions (with weight $c_j$) within, and between, molecules in the crystal structure. The last term, $L$, by the method of Lagrange multipliers, imposes such constraints as ring closure and helix connectivity. Comparison between competing molecular models at various stages of refinement can be made on the basis of $\Omega$, $X$, or $C$ by using Hamilton's significance test[15].

*Unit cell dimensions, helix symmetry, and feasible molecular models.* — The diffraction pattern shown in Fig. 2 contains 35 non-meridional and 3 meridional, sharp Bragg reflections extending to 0.3 nm resolution. These spots can be indexed on the basis of a trigonal unit cell with dimensions $a = b = 1.560(3)$ nm and

$c$ = 2.820(5) nm. The X-ray data set used in this analysis also includes 11 spots whose intensities are too weak to be measured, and a threshold value was assigned to each of them. Only those "below threshold" reflections for which the calculated structure amplitudes were higher than the corresponding observed values, were included in the least-squares refinement of the crystal structure.

Strong meridional spots on the 3rd, 6th, and 9th layer lines indicate that the molecules has 3n-fold helix symmetry. Because $c$ is only 2.82 nm, only 3-fold or 6-fold helices are sterically feasible. Both single- and double-helical models of both chiralities need to be examined. Two-dimensional, hard-sphere maps for the three sets of disaccharide units, namely Glc–Glc, Glc–Rha, and Rha–Glc, were calculated in order to determine the allowed domains of the two conformation angles ($\phi$, $\psi$) around the glycosidic bonds. These were used in generating the various helical models. At each linkage, the two glycosyl conformation angles were tethered to the values at the center of the corresponding allowed region.

Consistent with the layer-line spacings on the diffraction pattern, 3-fold single-helices of pitch 2.82 nm and 3-fold, as well as 6-fold, parallel, half-staggered, double-helices of pitch 5.64 nm were generated. The characteristics of these six possible models are listed in Table I. Four of them exhibit several over-short, intramolecular distances between nonbonded atoms, and are thus stereochemically not acceptable. The remaining two models do not suffer from any steric anomalies, and therefore are stereochemically satisfactory. These are the 3-fold, left-handed, single-helix (Model 2) and the 3-fold double-helix (Model 4) with left-handed chains. Structure factor calculations with two molecules in the unit cell (see next section for details) gave crystallographic $R$ values of 0.7 and 0.4 for Models 2 and 4, respectively. At this stage, we were able to ascertain the molecular structure of gellan to be a parallel, half-staggered, double-helix consisting of 3-fold, left-handed polytetrasaccharide chains of pitch 5.64 nm.

*Completion of the crystal structure.* — The measured density of the fiber is[5] 1.47 g/cc. This is consistent with two double-helices (Model 4) in the unit cell, together with at least one lithium ion for every carboxylate group, and ~25% (by

TABLE I

HELIX SYMMETRY AND CHARACTERISTICS OF SIX POSSIBLE POLYANION MODELS

| *Model* | *Helix* | *Type*[a] | *Chirality of chain* | *Pitch* (p) *(nm)* | *Steric feasibility*[b] |
|---|---|---|---|---|---|
| 1 | 3-fold single | — | right | 2.82 | SC |
| 2 | 3-fold single | — | left | 2.82 | good |
| 3 | 3-fold double | HS | right | 5.64 | SC |
| 4 | 3-fold double | HS | left | 5.64 | good |
| 5 | 6-fold double | HS | right | 5.64 | SC |
| 6 | 6-fold double | HS | left | 5.64 | SC |

[a]HS = parallel, half-staggered. [b]SC = some short contacts.

weight) of water molecules. The molecular axes must pass through the points (2/3, 1/3) and (1/3, 2/3) in the *ab* plane. The lowest symmetry possible is the space group $P3_1$. In this case, the molecular positions are specified by three packing parameters. These are the orientations of the two molecules about their long-axes $\mu_1$ and $\mu_2$, and the translation of the second molecule $w_2$ along it axis relative to the first. The two molecules may be parallel or antiparallel to each other. In the antiparallel case, if the two molecules are related by a dyad axis lying along the short cell diagonal [110], the number of independent packing variables is decreased to two ($\mu_2$ and $w_2$), and the space group becomes $P3_121$. There are neither systematic absences nor clues of any kind in the diffraction pattern which would enable us to distinguish between these three possibilities; only detailed refinement of the structures using X-ray amplitudes and contacts as observations can provide a definitive answer.

Using the molecular double-helix as a rigid body, we first determined the most probable values of the packing parameters $\mu_1$, $\mu_2$, and $w_2$ by conducting a survey of the crystallographic $R$ value, and the contact term $C$, in the three-dimensional space ($\mu_1$, $\mu_2$, $w_2$). Starting with these values, each crystal structure was refined by varying the packing parameters and the 12 conformation angles. The results of this analysis are summarized in Table II. The high symmetry space group $P3_121$ can be decisively eliminated with respect to both X-ray and contact data. The other two models (with space group $P3_1$), corresponding to the parallel and antiparallel packing, are equally good. They both have low values of $R$ (0.35 and 0.34) and are free from steric anomalies.

Attempts to locate the ordered lithium ions or water molecules by using difference-Fourier syntheses were unsuccessful. However, the contributions of disordered counter-ions and water molecules to the X-ray intensities can be approximated by choosing an appropriate solvent electron density used in the water (or solvent)-smeared atomic scattering factors[14]. This was done empirically by investigating the influence of varying the effective solvent electron density on the X-ray fit. By refining only the X-ray scale factor, $R$ was surveyed at discrete values of $\sigma$, ranging from 0 to 2.0, where $\sigma = 1$ corresponds to the interstitial space filled with a continuum of water (of electron density 298.4 e/nm$^3$). For both packings, the

TABLE II

STATISTICS FOR THE THREE COMPETING PACKING ARRANGEMENTS OF TWO 3-FOLD DOUBLE-HELICES IN THE UNIT CELL[a]

| *No.* | *Space group* | *Relative sense of the molecules* | X | C | R |
|---|---|---|---|---|---|
| 1 | $P3_1$ | parallel | 58 | 117 | 0.35 |
| 2 | $P3_1$ | antiparallel | 43 | 140 | 0.34 |
| 3 | $P3_121$ | antiparallel | 87 | 162 | 0.44 |

[a] $X$ and $C$ are the terms in Eq. *1* in arbitrary units, and $R$ is the crystallographic reliability index.

TABLE III

CARTESIAN AND CYLINDRICAL POLAR COORDINATES FOR A TETRASACCHARIDE ASYMMETRIC UNIT IN ONE CHAIN OF THE MOLECULAR DOUBLE-HELIX OF GELLAN[a]

| GROUP | ATOM | X(NM) | Y(NM) | Z(NM) | R(NM) | PHI(DEG) |
|---|---|---|---|---|---|---|
| RESIDUE A | C1 | -0.1258 | -0.3368 | 1.5102 | 0.3595 | -110.48 |
| | C2 | -0.1262 | -0.2882 | 1.6546 | 0.3147 | -113.65 |
| | C3 | -0.1804 | -0.3942 | 1.7493 | 0.4335 | -114.59 |
| | C4 | -0.3149 | -0.4457 | 1.6997 | 0.5457 | -125.24 |
| | C5 | -0.3043 | -0.4881 | 1.5536 | 0.5752 | -121.94 |
| | C6 | -0.4372 | -0.5316 | 1.4956 | 0.6883 | -129.43 |
| | O1 | -0.0919 | -0.2301 | 1.4281 | 0.2477 | -111.76 |
| | O2 | 0.0060 | -0.2515 | 1.6922 | 0.2516 | -88.63 |
| | O3 | -0.1954 | -0.3385 | 1.8800 | 0.3908 | -120.00 |
| | O4 | -0.3566 | -0.5581 | 1.7768 | 0.6623 | -122.57 |
| | O5 | -0.2576 | -0.3782 | 1.4738 | 0.4576 | -124.26 |
| | O6 | -0.4854 | -0.6509 | 1.5574 | 0.8120 | -126.72 |
| | H1 | -0.0566 | -0.4218 | 1.5003 | 0.4256 | -97.65 |
| | H2 | -0.1885 | -0.1979 | 1.6627 | 0.2733 | -133.60 |
| | H3 | -0.1083 | -0.4773 | 1.7529 | 0.4894 | -102.79 |
| | H4 | -0.3904 | -0.3663 | 1.7095 | 0.5353 | -136.82 |
| | H5 | -0.2341 | -0.5724 | 1.5449 | 0.6184 | -112.25 |
| | H61 | -0.5110 | -0.4511 | 1.5086 | 0.6816 | -138.56 |
| | H62 | -0.4264 | -0.5481 | 1.3874 | 0.6944 | -127.88 |
| RESIDUE B | C1 | 0.0397 | -0.1549 | 1.0390 | 0.1599 | -75.62 |
| | C2 | -0.0803 | -0.2478 | 1.0521 | 0.2604 | -107.96 |
| | C3 | -0.1403 | -0.2519 | 1.1918 | 0.2884 | -119.12 |
| | C4 | -0.0343 | -0.2589 | 1.3009 | 0.2611 | -97.54 |
| | C5 | 0.0760 | -0.1569 | 1.2745 | 0.1743 | -64.16 |
| | C6 | 0.1888 | -0.1654 | 1.3751 | 0.2510 | -41.22 |
| | O1 | 0.1041 | -0.1840 | 0.9194 | 0.2114 | -60.49 |
| | O2 | -0.1809 | -0.2079 | 0.9597 | 0.2756 | -131.04 |
| | O3 | -0.2255 | -0.3660 | 1.2040 | 0.4299 | -121.64 |
| | O4 | -0.0919 | -0.2301 | 1.4281 | 0.2477 | -111.76 |
| | O5 | 0.1325 | -0.1805 | 1.1446 | 0.2239 | -53.71 |
| | O61 | 0.1718 | -0.2410 | 1.4732 | 0.2959 | -54.52 |
| | O62 | 0.2904 | -0.0963 | 1.3524 | 0.3060 | -18.34 |
| | H1 | 0.0056 | -0.0505 | 1.0446 | 0.0508 | -83.67 |
| | H2 | -0.0505 | -0.3502 | 1.0254 | 0.3538 | -98.21 |
| | H3 | -0.2011 | -0.1617 | 1.2083 | 0.2580 | -141.19 |
| | H4 | 0.0085 | -0.3602 | 1.3020 | 0.3603 | -88.65 |
| | H5 | 0.0339 | -0.0553 | 1.2791 | 0.0649 | -58.53 |
| RESIDUE C | C1 | 0.1612 | -0.0758 | 0.5290 | 0.1782 | -25.17 |
| | C2 | 0.1516 | 0.0423 | 0.6246 | 0.1574 | 15.60 |
| | C3 | 0.1718 | -0.0089 | 0.7664 | 0.1720 | -2.96 |
| | C4 | 0.0660 | -0.1125 | 0.8021 | 0.1304 | -59.58 |
| | C5 | 0.0504 | -0.2157 | 0.6910 | 0.2215 | -76.84 |
| | C6 | -0.0797 | -0.2926 | 0.7005 | 0.3032 | -105.23 |
| | O1 | 0.1459 | -0.0314 | 0.3982 | 0.1492 | -12.15 |
| | O2 | 0.2491 | 0.1398 | 0.5890 | 0.2856 | 29.30 |
| | O3 | 0.1644 | 0.1003 | 0.8583 | 0.1926 | 31.38 |
| | O4 | 0.1041 | -0.1840 | 0.9194 | 0.2114 | -60.49 |
| | O5 | 0.0502 | -0.1608 | 0.5583 | 0.1685 | -72.66 |
| | O6 | -0.1923 | -0.2053 | 0.7085 | 0.2813 | -133.13 |
| | H1 | 0.2550 | -0.1312 | 0.5443 | 0.2868 | -27.23 |
| | H2 | 0.0530 | 0.0899 | 0.6144 | 0.1043 | 59.49 |
| | H3 | 0.2716 | -0.0544 | 0.7751 | 0.2770 | -11.33 |
| | H4 | -0.0293 | -0.0607 | 0.8201 | 0.0674 | -115.79 |
| | H5 | 0.1331 | -0.2881 | 0.6963 | 0.3173 | -65.20 |
| | H61 | -0.0901 | -0.3580 | 0.6127 | 0.3692 | -104.13 |
| | H62 | -0.0774 | -0.3577 | 0.7891 | 0.3660 | -102.21 |
| RESIDUE D | C1 | 0.4323 | 0.0797 | 0.1079 | 0.4396 | 10.44 |
| | C2 | 0.3201 | 0.1768 | 0.1426 | 0.3657 | 28.91 |
| | C3 | 0.2038 | 0.1045 | 0.2089 | 0.2290 | 27.15 |
| | C4 | 0.2549 | 0.0331 | 0.3332 | 0.2571 | 7.41 |
| | C5 | 0.3638 | -0.0663 | 0.2901 | 0.3698 | -10.32 |
| | C6 | 0.4302 | -0.1370 | 0.4067 | 0.4515 | -17.66 |
| | O1 | 0.3908 | 0.0000 | 0.0000 | 0.3908 | 0.00 |
| | O2 | 0.3741 | 0.2756 | 0.2294 | 0.4646 | 36.38 |
| | O3 | 0.1049 | 0.2017 | 0.2369 | 0.2274 | 62.52 |
| | O4 | 0.1459 | -0.0314 | 0.3982 | 0.1492 | -12.15 |
| | O5 | 0.4697 | 0.0014 | 0.2202 | 0.4697 | 0.17 |
| | H1 | 0.5195 | 0.1362 | 0.0718 | 0.5371 | 14.69 |
| | H2 | 0.2846 | 0.2260 | 0.0509 | 0.3634 | 38.46 |
| | H3 | 0.1618 | 0.0307 | 0.1388 | 0.1647 | 10.75 |
| | H4 | 0.2994 | 0.1074 | 0.4011 | 0.3181 | 19.73 |
| | H5 | 0.3201 | -0.1418 | 0.2232 | 0.3501 | -23.89 |
| | H61 | 0.3737 | -0.2281 | 0.4314 | 0.4378 | -31.40 |
| | H62 | 0.5333 | -0.1641 | 0.3793 | 0.5579 | -17.10 |
| | H63 | 0.4319 | -0.0701 | 0.4941 | 0.4376 | -9.22 |

[a]The next two tetrasaccharides in the chain have the coordinates ($R$, $\phi - 120°$, $Z + 2c/3$), and ($R$, $\phi + 120°$, $Z + 4c/3$). The second chain in the double-helix can be generated from the first by adding $c$ to the corresponding $Z$-coordinates. The asymmetric unit of the "down" molecule (see Table IV) will have ($R$, $-\phi$, $-Z$) for its atomic coordinates.

TABLE IV

STRUCTURE AMPLITUDES (*a*) SCALED OBSERVED AND (*b*) CALCULATED FOR THE ANTIPARALLEL PACKING OF DOUBLE-HELICES IN OUR BEST MODEL[a]

***a***

| H | K | L=0 | 1 | 2 | 3 | 4 | 5 | 6 | 7 | 8 | 9 |
|---|---|---|---|---|---|---|---|---|---|---|---|
| 0 | 0 | M | N | N | M | N | N | M | N | N | M |
| 1 | 0 | 164 | 101 | 48 | 23 | 59 | 106 | 71 | 121 | 143 | |
| 1 | 1 | 169 | 89 | (29) | 78 | 67 | 103 | 48 | 78 | | |
| 2 | 0 | 81 | 51 | 90 | (34) | (36) | (37) | 106 | (43) | 212 | |
| 2 | 1 | 343 | 264 | 130 | 108 | 139 | 138 | 148 | 106 | | |
| 3 | 0 | 376 | 301 | 173 | (50) | (52) | (55) | (58) | | | |
| 2<br>3 | 2<br>1 | 542 | 483 | 340 | | | | | | | |
| 4 | 0 | (72) | (71) | | | | | | | | |

***b***

| H | K | L=0 | 1 | 2 | 3 | 4 | 5 | 6 | 7 | 8 | 9 |
|---|---|---|---|---|---|---|---|---|---|---|---|
| 0 | 0 | (154) | 0 | 0 | (14) | 0 | 0 | (34) | 0 | 0 | (120) |
| 1 | 0 | 125 | 143 | 24 | 100 | 85 | 89 | 28 | 88 | 138 | |
| 1 | 1 | 143 | 134 | (64) | 105 | 45 | 108 | 94 | 76 | | |
| 2 | 0 | 132 | 37 | 112 | (43) | (34) | (87) | 123 | (41) | 201 | |
| 2 | 1 | 341 | 266 | 194 | 106 | 119 | 132 | 179 | 149 | | |
| 3 | 0 | 372 | 237 | 116 | (137) | (77) | (67) | (91) | | | |
| 2<br>3 | 2<br>1 | 479 | 449 | 312 | | | | | | | |
| 4 | 0 | (115) | (118) | | | | | | | | |

[a]The crystal structure can be derived from the molecular coordinates (see Table III) by applying the packing parameters $\mu_1$ for the "up" and ($\mu_2$, $w_2$) for the "down" molecules in the unit cell, 46.8° and (−11.2°, −0.1480), respectively. Amplitudes in parentheses indicate reflections below the threshold of observation, and their estimated threshold values are given in (*a*). Such reflections were included in the refinement only when their calculated values exceeded the threshold. M and N denote meridional and systematically absent reflections, respectively. An overall scale factor and an isotropic attenuation factor [$\exp(-0.06 \sin^2\theta/\lambda^2)$, where $\lambda = 0.15418$ nm] was applied to the calculated amplitudes.

X-ray fit was better ($R = \sim 0.27$) at $\sigma = 1.45$ than at the other values examined. This suggests that the effective electron density of the solvent in the gellan fiber is approximately 1.45 times that of water alone. Final rounds of refinement were subsequently conducted with $\sigma = 1.45$, and the conformations of the pyranose rings were also allowed to vary. The crystal structure of the antiparallel packing model

converged to a final $R$ value of 0.22, and the parallel packing model to a value of 0.24. Thus, the packing model which best fits all the data, restraints, and constraints is the one with the two double helices of the opposite sense. However, the superiority is not such as to exclude utterly the possibility that all the double helices have the same sense.

The atomic coordinates of the double-helix in the final model are given in Table III. The observed and calculated structure amplitudes are listed in Table IV.

*Morphology of the double-helix. — (a) Conformation.* The gellan polysaccharide chain is a 3-fold, left-handed helix. The conformation angles around the glycosidic bridges and C-5–C-6 bonds are listed in Table V, along with those of Upstill *et al.*[5] for comparison. The shapes of the pyranose rings are all very close to the standard $^4C_1$ ($^1C_4$ for L-rhamnose) geometries ($\langle\Delta\theta\rangle = 3.9°$). All the endocyclic sugar bond-angles are also near to the expected values, as are the bond angles at the bridge oxygen atoms ($\langle\Delta\alpha\rangle = 1.2°$). The conformation of the double-helix is shown in Fig. 3. The molecule forms an extended, helical structure. The O-6 atoms of the hydroxymethyl groups in both D-glucosyl residues take up *gauche* positions with respect to the C-4 atom, such that the dihedral angle $\theta$ (C-4–C-5–C-6–O-6) is $-66°$ in residue A and 53° in residue C. Whereas O-6 of D-glucose A describes the periphery of the molecule at $r = 0.81$ nm, the other O-6 atom (of D-glucose C) is much closer to the helix axis at a radius of 0.28 nm. The carboxylate group is rotated by only $-8°$ with respect to the C-4–C-5–C-6 plane of the D-glucosyluronic residue.

The intrusion of a (1→3) linkage at α-L-rhamnose in the otherwise β-D-(1→4)-linked, cellulose-like chain leads to interesting features in the secondary

TABLE V

FINAL VALUES (AND ESD VALUES) OF THE MAJOR CONFORMATION ANGLES OF GELLAN IN OUR BEST MODEL, AND COMPARISON WITH THOSE OF UPSTILL *et al.*[5]

| *Conformation angle* | *Value (degrees)* | | *Comment* |
|---|---|---|---|
| | *This study* | *Upstill* et al.[5] | |
| $\phi_1$ (O-5D–C-1D–O-3A–C-3A) | −140 (3) | −131 | α-(1→3) |
| $\psi_1$ (C-1D–O-3A–C-3A–C-4A) | 105 (3) | −41 | α-(1→3) |
| $\chi_1$ (C-4A–C-5A–C-6A–O-6A) | −66 (10) | 63 | hydroxymethyl |
| $\phi_2$ (O-5A–C-1A–O-4B–C-4B) | −86 (3) | −68 | β-(1→4) |
| $\psi_2$ (C-1A–O-4B–C-4B–C-5B) | −140 (3) | −117 | β-(1→4) |
| $\chi_2$ (C-4B–C-5B–C-6B–O-61B) | −8 (5) | 67 | carboxylate |
| $\phi_3$ (O-5B–C-1B–O-4C–C-4C) | −150 (4) | −123 | β-(1→4) |
| $\psi_3$ (C-1B–O-4C–C-4C–C-5C) | −134 (3) | −159 | β-(1→4) |
| $\chi_3$ (C-4C–C-5C–C-6C–O-6C) | 53 (5) | 54 | hydroxymethyl |
| $\phi_4$ (O-5C–C-1C–O-4D–C-4D) | −168 (5) | −104 | β-(1→4) |
| $\psi_4$ (C-1C–O-4D–C-4D–C-5D) | 75 (4) | 133 | β-(1→4) |
| $\chi_4$ (C-4D–C-5D–C-6D–H-61D) | 88 (10) | 60 | methyl |

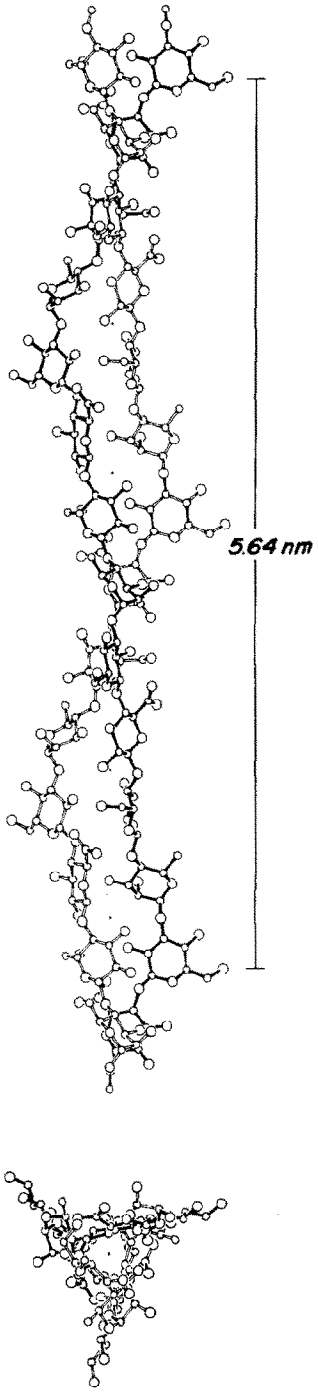


Fig. 3. Two mutually perpendicular views of the 3-fold double-helix. [One strand is shown in thick bonds for clarity.]

structure. Globally, the average turn angle per sugar residue about the helix-axis is −30°, but this angle is not uniformly distributed along the chain. The local turn angles, measured as the difference in cylindrical polar angle $\phi$ (see Table III) of adjacent bridge oxygen atoms, are high for D-glucuronate (−51°) and D-glucose C (−48°), and are accompanied by small turn angles for L-rhamnose (−12°) and D-glucose A (−8°). The corresponding, projected lengths of the adjacent bridge-oxygen atoms along the helix-axis follow a similar trend, namely, larger values for D-glucuronate (0.51 nm) and D-glucose C (0.52 nm) residues than for L-rhamnose (0.40 nm) and D-glucose A (0.45 nm). The average rise per sugar residue is 0.47 nm, and the dispersion is ~0.05 nm. In cellulose, which has the fully extended conformation, the axial rise is 0.52 nm. Inspection of the two pairs of conformation angles, ($\phi_2$, $\psi_2$) and ($\phi_3$, $\psi_3$), in Table V reveals that the values in the former are remarkably similar to those (−98°, −142°) reported for the crystal structure of cellulose[16]. In the second pair, only $\phi_3$ differs significantly (by about −52°) from that of cellulose.

*(b) Intra-chain hydrogen bonds.* The slim, gellan chain derives stability through three intramolecular hydrogen-bonds per tetrasaccharide unit, all of them involving the D-glucuronate residue (see Table VI) across the bridge-oxygen atoms (see Fig. 4). As in the structure of cellulose, the hydrogen bond O-3B···O-5A is noteworthy. The other two are O-2A···O-61B and O-2B···O-6C. The distances and angles of the hydrogen bonds are satisfactory (see Table VI). The hydroxyl groups in the L-rhamnosyl residue do not participate in any hydrogen bonds within the chain.

*(c) Inter-chain hydrogen bonds.* The double-helix is stabilized by three OH···O hydrogen bonds (see Table VI), involving the D-glucuronate B residue as the acceptor and D-glucose C and L-rhamnose D residues as the donors. The donor and acceptor groups are in the interior of the molecule, and are situated close to the helix-axis at radial distances of between 0.23 and 0.31 nm. As a donor, O-6C forms bifurcated hydrogen bonds with O-61B and O-62B. Simultaneously, O-3D hydrogen-bonds to O-2B.

TABLE VI

HYDROGEN BONDS WITHIN THE DOUBLE HELIX

| *Type* | *Donor* X | *Acceptor* Y | *Distance (nm)* | *Precursor* P | *Angle (degrees)* P–X···Y |
|---|---|---|---|---|---|
| Intrachain | O-3B | O-5A | 0.272 | C-3B | 101 |
| Intrachain | O-2A | O-61B | 0.275 | C-6B | 111 |
| Intrachain | O-2B | O-6C | 0.251 | C-2B | 133 |
| Interchain | O-6C | O-61B | 0.269 | C-6C | 132 |
| Interchain | O-6C | O-62B | 0.298 | C-6C | 93 |
| Interchain | O-3D | O-2B | 0.297 | C-3D | 117 |

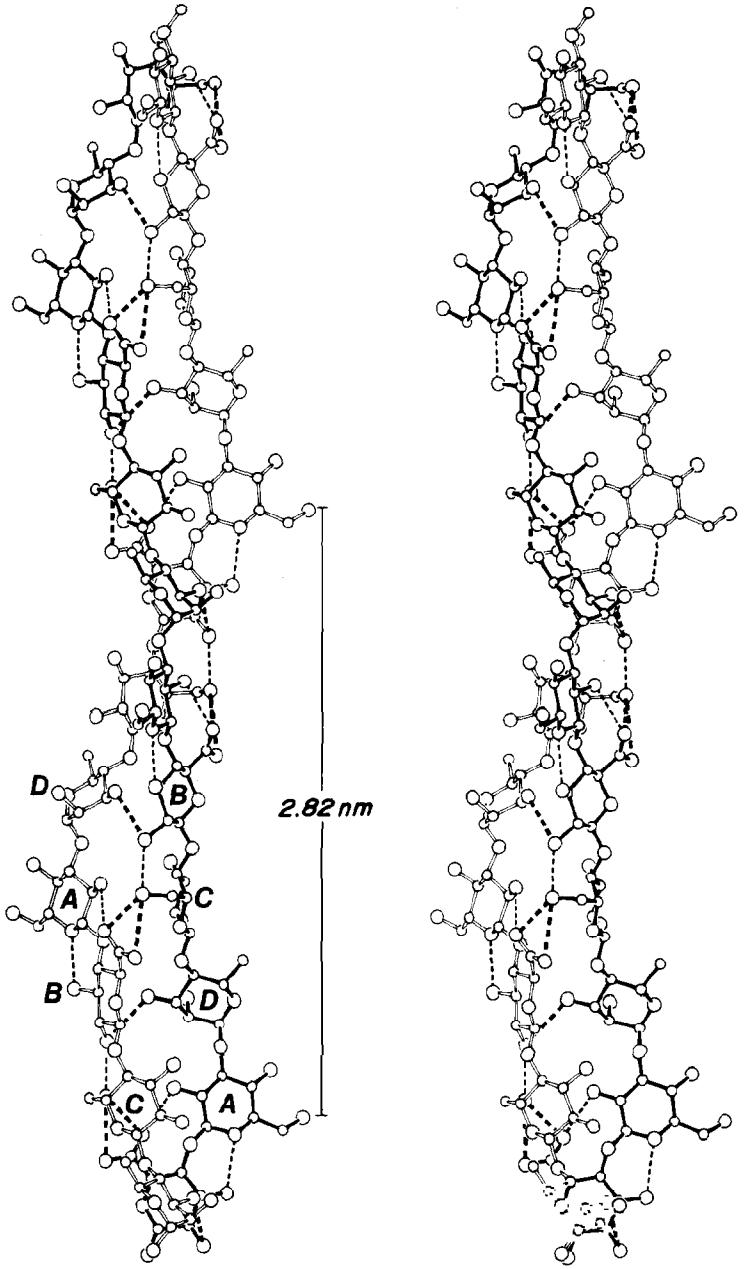


Fig. 4. Side view of the double helix in stereo showing the OH···O hydrogen bonds within the molecule. [Intrachain interactions O-3B···O-5A, O-2A···O-61B, and O-2B···O-6C are indicated by thin, dashed lines. Interchain interactions O-6C···O-61B, O-6C···O-62B, and O-3D···O-2B are indicated by thick, dashed lines.]

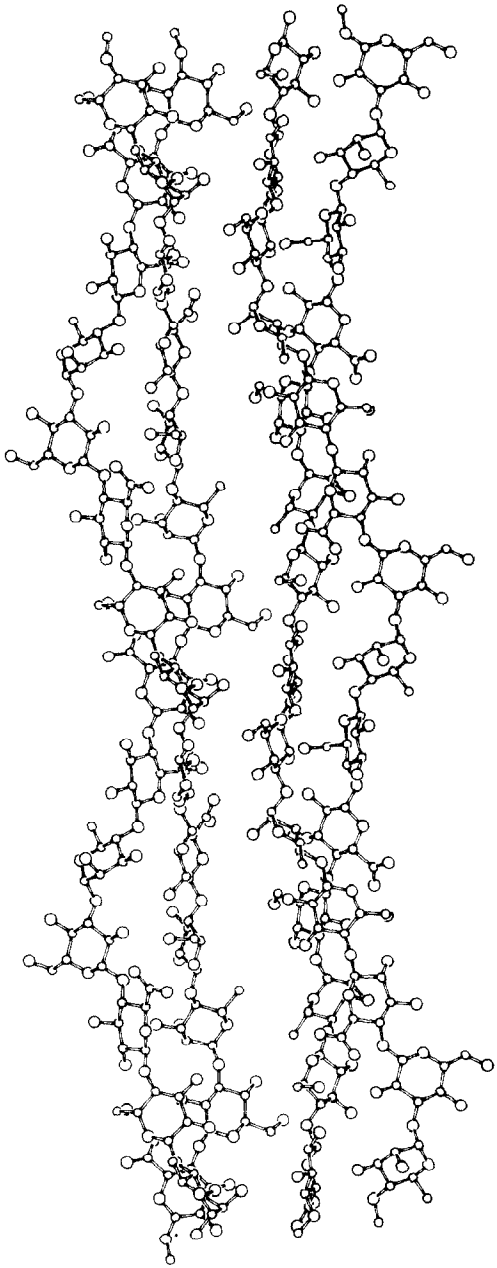

Fig. 5. Packing of two adjacent, up and down, molecules as viewed along the [110] direction of the unit cell.

*Interactions between double helices.* — The two double-helices in the unit cell may be packed parallel or antiparallel. The resulting crystal structures are both acceptable, and cannot be readily distinguished by the X-ray data used in this analysis. The interactions between molecules are similar in both cases. We have taken the antiparallel packing as being representative. A view of the two molecules along the [110] direction is shown in Fig. 5. Most of the intermolecular hydrogen bonds involve either the free hydroxyl groups of L-rhamnose or the hydroxymethyl group of D-glucose A, which is located farthest from the helix-axis. Each molecule in the unit cell interacts with its three nearest neighbors, which are laterally separated by 0.9 nm from it, as shown in Fig. 6.

*Comparison of our best model with that of Upstill and co-workers*[5]. — A detailed examination of the analysis of Upstill *et al.*[5] has now revealed that their erroneous results were due to incorrect structure factor calculations, leading to poor X-ray agreement. Their best model (see Table 2d in Upstill *et al.*[5]) is also a 3-fold double-helix with left-handed polysaccharide chains packed antiparallel in the unit cell. The conformation angles of their model are listed in Table V, along with our final model. The main chain conformation angles in the two cases are similar, with the exception of $\psi_1$, which shows a large difference of 146°. Consequently, the two molecular shapes are distinctly different. Forcing $\psi_1$ of our model to move into the *gauche*-minus domain during a proper X-ray-contact refinement of the crystal structure leads to an increase in the $R$ value to 0.38, indicating that this model is substantially inferior to ours.

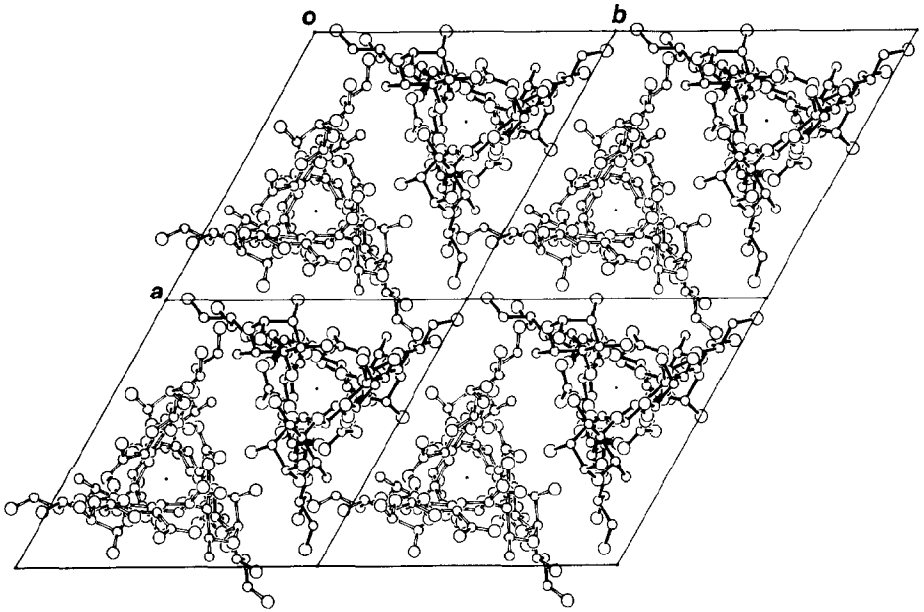


Fig. 6. Helix-axis projection of the crystal structure corresponding to the antiparallel packing arrangement. [The "down" molecules are drawn with thick bonds.]

## DISCUSSION

It is of no little interest that the gellan molecule forms a parallel, half-staggered, double-helix that is similar to that reported for the other gel-forming polysaccharides ι-carrageenan[7] and agarose[8]. Each chain has left-handed, 3-fold helix symmetry, and displays an extended cellulose-like conformation. The carboxylate group of D-glucuronate B, and the D-glucose C and L-rhamnose D residues are engaged in interchain interactions which stabilize the double-helix. Similarly, the free hydroxyl groups of L-rhamnose and the hydroxymethyl groups of D-glucose A residues are involved in hydrogen bonds between the double-helical molecules.

It is likely that the gelling mechanism of gellan is based on the formation of double-helical junction-zones, followed by aggregation of the double-helical segments, which lead to a three-dimensional network, as proposed for other gel-forming polysaccharides[17]. Native gellan, as secreted by the micro-organism, is always acetylated, and forms only weak gels. On the other hand, deacetylation promotes gel formation. Kuo *et al.*[18] recently established that the acetylation occurs only on O-6 of D-glucose A. Our structural results suggest that acetylation of D-glucose A will not disrupt double-helix formation, but that the aggregation of the molecules will be somewhat lessened, compared to the deacetylated material. Hence, acetylation would be expected to lessen, rather than completely abolish, gel-forming properties, resulting in a weaker gel, as is observed[19].

## ACKNOWLEDGMENTS

We thank Julie Sommers for word-processing the manuscript, Robert Werberig for photography, and the National Science Foundation for financial support (Grants 8512599 and 8606942).

## REFERENCES

1 M. A. O'NEILL, R. R. SELVENDRAN, AND V. J. MORRIS, *Carbohydr. Res.*, 124 (1983) 123–133.
2 P. E. JANSSON, B. LINDBERG, AND P. A. SANDFORD, *Carbohydr. Res.*, 124 (1983) 135–139.
3 V. CARROLL, M. J. MILES, AND V. J. MORRIS, *Int. J. Biol. Macromol.*, 4 (1982) 432–433.
4 V. CARROLL, G. R. CHILVERS, D. FRANKLIN, M. J. MILES, V. J. MORRIS, AND S. G. RING, *Carbohydr. Res.*, 114 (1983) 181–191.
5 C. UPSTILL, E. D. T. ATKINS, AND P. T. ATTWOOL, *Int. J. Biol. Macromol.*, 8 (1986) 275–288.
6 P. J. C. SMITH AND S. ARNOTT, *Acta Crystallogr., Sect. A*, 34 (1978) 3–11.
7 S. ARNOTT, W. E. SCOTT, D. A. REES, AND C. G. A. MCNAB, *J. Mol. Biol.*, 90 (1974) 253–267.
8 S. ARNOTT, A. FULMER, W. E. SCOTT, I. C. M. DEA, R. MOORHOUSE, AND D. A. REES, *J. Mol. Biol.*, 90 (1974) 269–284.
9 R. P. MILLANE AND S. ARNOTT, *J. Appl. Crystallogr.*, 18 (1985) 419–423.
10 R. P. MILLANE AND S. ARNOTT, *J. Macromol. Sci. Phys., Sect. B*, 24 (1985) 193–227.
11 S. ARNOTT AND W. E. SCOTT, *J. Chem. Soc. Perkin Trans. II*, (1972) 324–335.
12 S. TAKAGI AND G. A. JEFFREY, *Acta Crystallogr., Sect. B*, 34 (1978) 2551–2555.
13 *International Tables for X-Ray Crystallography*, Vol. IV, 1974, Kynoch Press, Birmingham, England.

14 S. ARNOTT, R. CHANDRASEKARAN, A. W. DAY, L. C. PUIGJANER, AND L. W. WATTS, *J. Mol. Biol.*, 149 (1981) 489–505.
15 W. C. HAMILTON, *Acta Crystallogr.*, 18 (1965) 502–510.
16 K. H. GARDNER AND J. BLACKWELL, *Biopolymers*, 13 (1974) 1975–2001.
17 D. A. REES, I. W. STEELE, AND F. B. WILLIAMSON, *J. Polym. Sci., Part C*, (1969) 261–276.
18 M. S. KUO, A. DELL, AND A. J. MORT, *Carbohydr. Res.*, 166 (1986) 173–187.
19 G. R. SANDERSON AND R. C. CLARK, *Food Technol.*, 37 (1983) 63–70.